ELSEVIER

Journal of Alloys and Compounds 287 (1999) 12–17

Journal of ALLOYS AND COMPOUNDS

Short-range order in a thin film of decagonal Al–Co–Ni quasicrystal: calculated from a structure model and measured with EXAFS

Stefan Braun[a], Dirk C. Meyer[a], Peter Paufler[a,*], Benjamin Grushko[b]

[a]*Institut für Kristallographie und Festkörperphysik, Fachrichtung Physik, Technische Universität Dresden, D-01 062 Dresden, Germany*
[b]*Institut für Festkörperforschung, Forschungszentrum Julich GmbH, D-52425 Jülich, Germany*

Received 26 October 1998

Abstract

Extended X-ray Absorption Fine Structure (EXAFS) measurements performed at the Co and Ni K absorption edges of thin decagonal $Al_{73}Co_{16}Ni_{11}$ quasicrystalline films are presented. Layers were grown by solid state reaction of a multilayer stack of elemental metals. Experimental data of short range order is compared to that calculated from a modified Li–Steurer structure model. To fit the measured EXAFS function, the neighbourhood of transition metals cobalt and nickel up to 3 Å was calculated from this model. Overlap of hyperatoms in the perpendicular space has been taken into account. The algorithm for the calculation of the average neighbourhood of a given element can also be applied to other quasicrystalline structures modelled by using a cut-and-projection method from a high-dimensional space. The average neighbourhood of Ni and Co atoms was found to be equal within a radius of 3 Å. Sites of transition metals should be occupied statistically by Ni and Co.

Keywords: Al–Co–Ni alloys; Quasicrystal; Thin film; EXAFS

1. Introduction

Both stability and structure of the decagonal phase in the system Al–Co–Ni has been studied by a number of workers [1–7]. Nevertheless, many problems remain to be solved due to a pronounced effect of composition and temperature on structure [2,3,5–7]. In view of the lack of periodicity in two dimensions experimental data on short range order should help to refine the structure. For this purpose we have probed just the local structure using extended X-ray absorption fine structure (EXAFS). So far, relatively few authors have applied EXAFS to work out details of the quasicrystalline structure (e.g. in the systems Al–Mn [8], Al–Mn–Si [9], Al–Li–Cu [10,11], Al–Pd–Re, Al–Pd–Mn [12], Al–Cu–Fe [13], Al–Cu–Co [14]). One reason for this is probably the difficulty of obtaining atom coordinates in real space. In the present case of a decagonal quasicrystal this requires projection of a five-dimensional space with the occupation domain extended to the two-dimensional space [15].

Recently, much effort has been made to prepare quasicrystalline films. For a couple of years it appeared that only binary quasicrystalline phases could be grown by annealing of multilayer stacks [16]. It was only very recently that films of a decagonal phase in the ternary system Al–Cu–Co have successfully been prepared [17]. To our knowledge, thin films of Al–Co–Ni d-phase have hitherto not yet been obtained.

It is the aim of this paper to communicate for the first time results of an EXAFS study of the Al–Co–Ni d-phase at both the Co and Ni K-edges and compare them with the radial distribution around Co and Ni atoms as derived from a structural model.

2. Modelling of neighbourhood

Let us first deal with the way we adopted structure geometry. The structure of the decagonal phase of Al–Ni–Co has a periodicity along its ten-fold axis and a two-dimensional quasiperiodicity perpendicular to this axis. Depending on composition and temperature various structure modifications and superstructures have been observed so far [2,3,5–7,18].

In this paper we will make use of the structural model as proposed by Steurer et al. [1] which is an idealisation without any superordering. It was derived using refined

*Corresponding author.
E-mail address: paufler@physik.phy.tu-dresden.de (P. Paufler)

0925-8388/99/$ – see front matter
PII: S0925-8388(98)01058-5

diffraction data of decagonal $Al_{70}Ni_{15}Co_{15}$. According to this model the structure consists of two quasiperiodic periodically repeated layers where one layer is a copy of the other rotated by 36°. However, this model still contains aluminum atoms with interatomic distances of 2.25 Å which are much smaller than expected for metallic radii (~2.86 Å). Therefore, we have used a modified model as put forward by Deus [19] in which these short distances do not occur any longer.

The structure description can be obtained by decorating a five-dimensional hyperrhombic lattice [1] with hyperatoms. The five-dimensional lattice is subdivided into parallel and perpendicular space, in which the parallel space represents the physical space (three-dimensional). The hyperatoms are extended along the perpendicular space (two-dimensional). If the parallel space intersects a hyperatom, this atom originates from the real space. The kind of this atom, whether aluminum or transition metal, depends on the area in which the hyperatom was intersected.

Consider two hyperatoms at $\vec{r}_1$ and $\vec{r}_2$ in the five-dimensional space. The distance between $\vec{r}_1$ and $\vec{r}_2$ projected onto the parallel and perpendicular space is d_{par} and d_{perp}, respectively. Only if there is an overlap in the perpendicular space of both hyperatoms both atoms can appear in the real space simultaneously. The necessary condition is that the distance d_{perp} of the two hyperatoms is less than the largest extension of the hyperatoms. The distance of the two atoms in real space is then d_{par}. To obtain the neighbourhood up to distances of 3 Å of transition metals one has to choose hyperatoms which yield a transition metal and to calculate the overlap of these hyperatoms with all other atoms at a distance $d_{par}<3$ Å. As seen from the decoration of hyperatoms (Fig. 1) a transition metal atom (TM) can arise if the parallel space intersects hyperatom 1 or 3. The section of hyperatom 1 leads to an atom in real space in – let us say – a layer A, whereas the section of hyperatom 3 leads to an atom in a neighboured layer B, which is twisted by 36° relative to layer A. The two layers A and B are symmetrically equivalent. The average neighbourhood of atoms in layer A is the same as for atoms in layer B. Therefore, it is sufficient to consider the overlap of hyperatoms of type 1 with all other hyperatoms to get the average next neighbourhood of transition metals. Restricting the distance d_{par} to 3 Å, the result is that the central hyperatom 1 overlaps with ten hyperatoms 1 ($d_{par}=2.88$ Å), with five hyperatoms 2 ($d_{par}=2.46$ Å), with five hyperatoms 3 ($d_{par}=2.54$ Å) and with five hyperatoms 4 ($d_{par}=2.54$ Å). When calculating the number of neighbouring atoms at the shortest distance of 2.46 Å one has to consider the overlap of the central hyperatom 1 with the five hyperatoms 2 (Fig. 2). Because of the symmetry of the overlap, it is sufficient to calculate the six polygons inside the asymmetrical unit of overlap. Contribution of a patch i to the number of neighbours of the sort B around a central atom of sort A is given by:

$$N^i_{A,B} = \frac{F^i w^i_A}{\sum_k F^k w^k_A} \sum_j w^i_{B,j} \quad (1)$$

F^i is the size of overlap i, w^i_A is the probability that with the cross-section of patch i of central hyperatom an atom of sort A is formed, k is a control variable over all patches of central hyperatom which could lead to an atom of type A, j is a control variable over all neighbouring hyperatoms, which cover the subrange i and $w^i_{B,j}$ is the probability that with the cross-section of hyperatom j in patch i an atom of type B is formed.

In the present case of hyperatoms 2 we have A = transition metal = TM and B = Al. If the overlap of hyperatom 1 and hyperatoms 2 is considered, the probabilities $w^i_{Al,j}$ are 0 or 1 depending on whether hyperatom

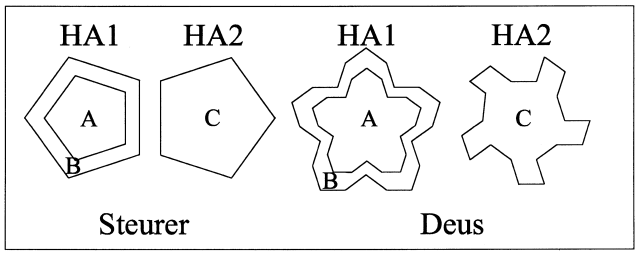

Fig. 1. Shape and decoration of hyperatoms used according to Steurer et al. [1] and Deus [19]. The decoration of hyperatoms of Deus was performed analogously to the decoration of Steurer's hyperatoms under the condition that $n_{AL}:n_{TM}=70:30$. The hyperatoms 3 and 4 not shown here are identical to hyperatoms 1 and 2, just rotated by 36°. Region A yields a transition metal atom in real space, region B and C yield aluminum atoms. According to Steurer et al. [1] transition metal atom sites are considered to be randomly occupied by cobalt or nickel.

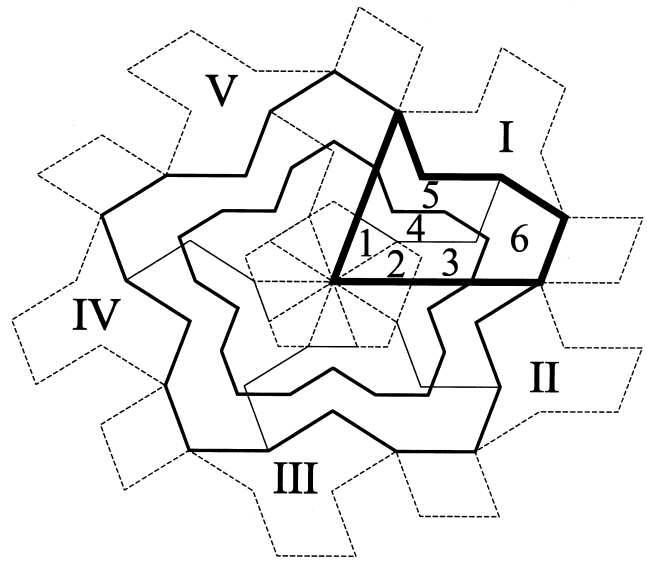

Fig. 2. Overlap of the central hyperatom 1 and the hyperatoms 2 projected on the perpendicular space according to the model of Deus [19]. The bold polygon marks the asymmetric unit of the overlap.

2 covers the patch i or not. Cross-sections with the different patches lead to the following neighbourhoods: area 1: 4 neighbouring Al atoms (overlap of hyperatom 1A and hyperatoms 2I, 2II, 2III, 2V), area 2: 3 Al atoms (2I, 2II, 2III), area 3: 2 Al atoms (2I, 2II) area 4: 2 Al atoms (2I, 2V), area 5: 1 Al atom (2I) and area 6: 2 Al atoms (2I, 2II). Evaluating the size of the patches and then summing up the average number of Al atoms around TM atoms due to hyperatoms 2 the corresponding coordination number becomes $N_{\mathrm{TM,Al}} = \Sigma_i N^i_{\mathrm{TM,A1}} = 3.28$. The same procedure has been applied to all other hyperatoms.

3. Experimental

We now turn to the experimental part. The sample considered here was prepared by annealing of elemental multilayers deposited by pulsed laser deposition (PLD) [20]. The multilayer consisted of ten periods of the sequence Co/Al/Ni, where the first cobalt layer was deposited on a (012) sapphire substrate. The mean thicknesses of the layers were $d_{\mathrm{Al}} \approx 15$ nm, $d_{\mathrm{Co}} \approx 2.2$ nm and $d_{\mathrm{Ni}} \approx 1.8$ nm as determined by X-ray reflectometry [21]. From stack geometry the overall composition was determined to be $Al_{73}Co_{16}Ni_{11}$. After annealing at 700°C for 5 h with a heating rate of 1 K/mm and at a pressure less than 2×10^{7}mbar the single-phase decagonal structure was formed by solid state reaction. All reflections of the X-ray diffraction pattern (Fig. 3) can be indexed on base of the decagonal quasicrystalline phase [22]. Moreover, comparison with a pattern of a quasicrystalline powder sample $Al_{72}Co_{125}Ni_{155}$ shows good agreement (Fig. 3). However, a strong preferred orientation with periodic direction aligned perpendicular to the surface of substrate can be stated (Fig. 4). The 00002 reflection, representing the periodic direction, is very sharp having high intensity

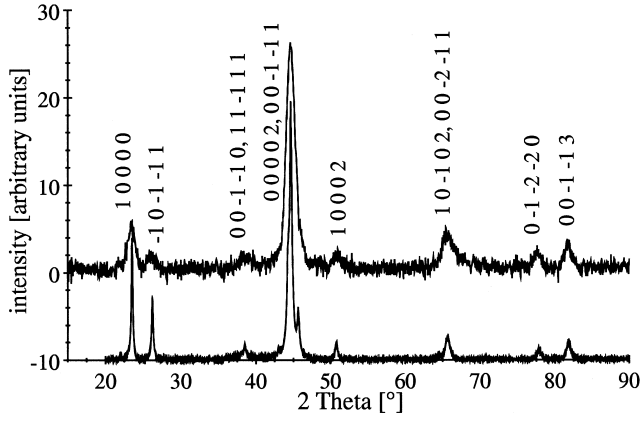

Fig. 3. Diffraction pattern of the quasicrystalline thin film obtained with asymmetrical scan at fixed angle of incidence $\omega = 2°$. CuKα and a Si-(111) monochromator were used. Indexing according to to Kek and Meyer [22]. Long axis of the rectangular sample perpendicular to diffraction plane.

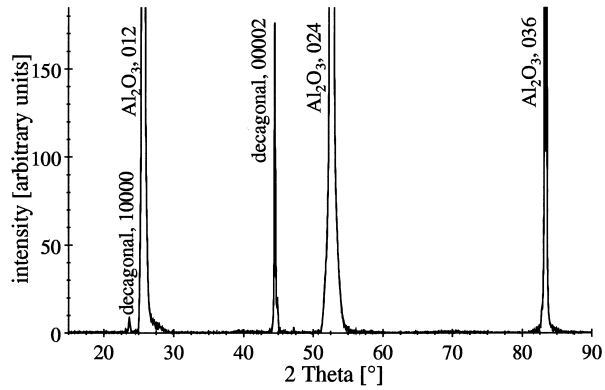

Fig. 4. Diffraction pattern of the symmetrical ω-2θ scan of the quasicrystalline thin film. The sharp and intensive 00002 peak at 44.6° indicates the alignment of the periodic direction perpendicular to the substrate surface.

compared to that of the further decagonal reflection 10000. From a rocking scan of this 00002 reflection a half width of 0.114° was obtained.

EXAFS measurements were carried out at the Hamburger Synchrotron Strahlungslabor (HASYLAB). (For set-up, see Ref. [23]). Measurements were carried out at Co and Ni K absorption edges, respectively. Because of the substrate (sapphire wafer with thickness of 500 μm), the usual way to measure the absorption coefficient by transmission was not applicable. Therefore the fluorescence intensity was measured to obtain the absorption coefficient $\mu(E) = \mu_0(E)(1 + \chi(E))$ for EXAFS. E is the energy of incident X-ray photons, $\mu_0(E)$ is the absorption coefficient of free atoms without contributions of neighbours. $\chi(E)$ is the characteristic EXAFS function. This function was compared with results obtained from measurements at a quasicrystalline reference powder sample of composition $Al_{72}Co_{12.5}Ni_{15.5}$. As can be seen in Fig. 5, both functions χ agree well.

4. Results and discussion

Fourier transformation of $k \cdot \chi(k)$ reveals that mainly atoms at distances up to 3 Å to the absorbing atom contribute to the EXAFS signal. The backtransformed range of the main peak gives a slightly changed function $\chi(k)$, which is the basic function for fitting the calculated χ to coordination numbers and distances obtained from the five-dimensional structure model. Assuming polycrystalline samples and ignoring contributions from multiple scattering and further weakenings, one has [24]

$$\chi(k) = \sum_j 3N_j(\vec{\epsilon} \cdot \vec{e}_j)^2 F_j(k)\, \mathrm{e}^{-2\sigma_j^2 k^2} \frac{\sin(2kr_j + \Phi_{ij}(k))}{kr_j^2} \qquad (2)$$

where k is the wave vector modulus of the emitted photoelectron. $F_j(k)$ is the backscattering amplitude from

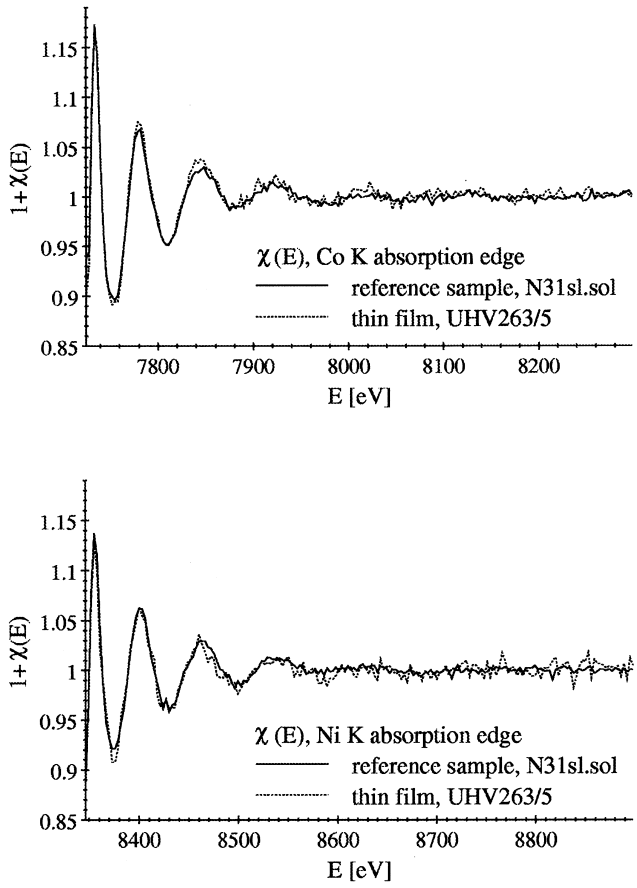

Fig. 5. Comparison of the EXAFS functions of the thin film and of the quasicrystalline reference sample at Co and Ni K absorption edge. High frequency oscillations of solid curve are probably due to the statistics of the small diffraction volume.

each of the N_j neighbouring atoms of type j with a Debye–Waller factor σ_j at $\vec{r}_j = r\vec{e}_j$ relative to the absorbing atom of the type i. Φ_{ij} is the total phase shift experienced by the photoelectron wave and $\vec{\epsilon}$ is the unit polarisation vector of the incident X-ray beam. Terms neglected here describe inelastic losses and amplitude attenuations by other influences. The calculation is based on data of McKale et al. [25], which contains the backscattering amplitudes and the phase shifts of the primary and the backscattered electron wave as function of energy.

In Eq. (2) the effective coordination number $N_{\text{eff}} = 3(\vec{\epsilon}\cdot\vec{\epsilon}_r)^2$ has to be calculated. Using grazing incidence the polarisation vector of X-rays was parallel to the substrate surface. Consequently, the polarisation vector lies also parallel to the quasiperiodic planes and can be written $\vec{\epsilon}=(\cos\alpha,\ \sin\alpha,\ 0)$, where α is the angle between $\vec{\epsilon}$ and the x-axis (z-axis parallel to the periodic direction). Assuming random orientation of aligned grains around the periodic ten-fold direction the effective coordination number has been averaged over the angle α. Replacing the unit radius vector $\vec{\epsilon}_r$ by $(\cos\phi\ \sin\vartheta,\ \sin\phi,\ \sin\vartheta,\ \cos\vartheta)$, where ϕ and ϑ are spherical coordinates, the averaged effective coordination number becomes:

$$N_{\text{eff}}{}^{\alpha} = \frac{1}{2\pi}\int_0^{2\pi} N_{\text{eff}}(\alpha,\phi,\vartheta)\mathrm{d}\alpha = \frac{3}{2}\sin^2\vartheta$$

Atoms, which lie in the same quasi-periodic plane as the absorbing atom, have to be weighted by a factor 1.5 ($\vartheta = 90°$). For atoms at distance $|\vec{r}| = 2.54$ Å lying in neighbouring layers we have $\vartheta = 36.64°$, i.e. $N_{\text{eff}}{}^{\alpha} = 0.534$. For other values see Table 1.

We have fitted the computed curve to the measured one by variation of energy shift ΔE_0 of the McKale data and of disorder parameter σ keeping coordination numbers Z and distances r constant. As shown in Fig. 6, a good fit to the measurement can be achieved. The fit is acceptable with spherical averaging as well as with averaging over the quasi-periodic plane for both models. Differences in coordination numbers can be compensated for by altering the disorder parameters σ. Final results of best fit are listed in Table 2.

Dong et al. [14] carried out EXAFS measurements of Al–Cu–Co similar to decagonal Al–Ni–Co. They reported that they were first unable to fit the experiments in the higher k-range. In this region both curves were out of phase. It was concluded that similarly to amorphous structures the partial radial distribution function is likely to be asymmetric and the Gaussian approximation in Eq. (2) is not valid. Therefore, they took lowest-order corrections into account. In the present work, we succeeded to fit the measurement without this correction. Unlike Ref. [14] we did not presuppose that TM atoms only have Al neighbours. TM neighbours were also considered. In the upper k-range the influence of the TM neighbours to the EXAFS

Table 1
Radial distribution of atoms around central TM atoms, spherically averaged (powder-like) and averaged over the quasiperiodical plane

Hyperatom	Atom	d_{par}	$N_{\text{spherical averaged}}$		N^{α}_{eff}	
origin	type		Steurer [1]	Deus [19]	Steurer [1]	Deus [19]
2	Al	2.46	3.28	2.56	4.92	3.84
3	Al	2.54	0.41	0.61	0.22	0.33
3	TM	2.54	0.61	0.67	0.33	0.36
4	Al	2.54	1.55	1.10	0.83	0.59
2	Al	2.88	0.61	0.98	0.91	1.47
2	TM	2.88	0.41	0.43	0.61	0.64

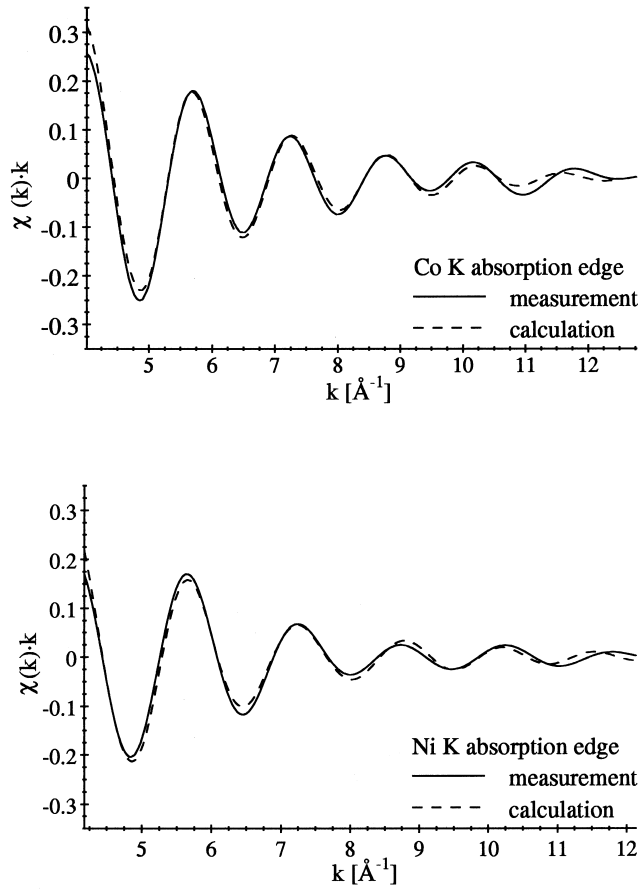

Fig. 6. Comparison of the measured and calculated best fit EXAFS function $\chi(k)\cdot k$ at the Co and Ni K absorption edge.

signal predominates, because the backscattering amplitude of Al has its maximum at 4 Å, whereas the backscattering amplitudes of TM atoms have its highest values at about 7 Å^{-1}. In addition, considering the total phase shift in the case of TM as absorbing atom, it can be recognised that the total phase shift changes by about π, if TM is the backscattering atom instead of aluminum. Hence, the computed function must also show a dephasing at higher k-values compared to lower ones.

5. Conclusion

From the present results we conclude that the average neighbourhood of Ni and Co atoms is equal within a radius of ~3 Å. Sites of transition metals are occupied statistically by Ni and Co. The radial distribution of atoms as proposed by the structural model of Steurer/Deus has been verified within a sphere of radius ~3 Å around TM atoms. Thus short-range order in thin films appears to be the same as in bulk quasicrystals.

Acknowledgements

We would like to thank Dr Rhena Krawietz for stimulating discussion. Financial support by the Deutsche Forschungsgemeinschaft and the Fonds der Chemischen Industrie is gratefully acknowledged.

References

[1] W. Steurer, T. Haibach, B. Zhang, S. Kek, R. Luck, Acta Crystallogr. B 49 (1993) 661.
[2] K. Edagawa, H. Tamaru, S. Yamaguchi, K. Suzuki, S. Takeuchi, Phys. Rev. B 50 (1994) 12413.
[3] B. Grushko, K. Urban, Philos. Mag. B 70 (1994) 1063.
[4] W. Würschum, T. Troev, B. Grushko, Phys. Rev. B 52 (1995) 6411.
[5] A. Baumgarte, J. Schreuer, M.A. Estermann, W. Steurer, Philos. Mag. A 75 (1997) 1665.
[6] B. Grushko, D. Holland-Moritz, J. Alloys Compd. 262–263 (1997) 350.
[7] B. Zhang, M. Estermann, W. Steurer, J. Mater. Res. 12 (1997) 2274.
[8] E.A. Stern, Y. Ma, C.E. Bouldin, Phys. Rev. Lett. 55 (1985) 2172.
[9] E.A. Stern, Y. Ma, Philos. Mag. Lett. 56 (1987) 103.
[10] Y. Ma, W.A. Stern, F.W. Gayle, Phys. Rev. Lett. 58 (1987) 1956.
[11] A. Sadoc, J.P. Itié, A. Polian, S. Lefebvre, J. Phys. IV France. 7 (1997) C2–991.
[12] A. Sadoc, J.S. Poon, M. Boudard, Quasicrystals, in: Proc. 5th Int. Conf., Avignon, World Scientific, Singapore, 1995, p. 156.
[13] J.P. Itié, S. Lefebvre, A. Sadoc, M.J. Capitan, M. Bessiere, Y. Calvayrac, A. Polian, Quasicrystals, in: Proc. 5th Int. Conf., Avignon, World Scientific, Singapore, 1995, p. 168.
[14] J. Dong, K. Lu, H. Yang, Q. Shan, Philos. Mag. B 64 (1991) 599.
[15] A. Yamamoto, K.N. Ishihara, Acta Crystallogr. A 44 (1988) 707.

Table 2
Fit parameters of the calculated EXAFS function $\chi(k)$ at Co and Ni K absorption edges using the model of Deus [19]. Values in braces indicate the results for spherical averaging

Atom type	$\bar{N}^{\alpha}_{eff}$ ($N_{\text{sph. av.}}$)	r/Å	Absorption atom: Co		Absorption atom: Ni	
			σ^2/Å^2	ΔE_0/eV	σ^2/Å^2	ΔE_0/eV
Al	3.84 (2.56)	2.46	0.004 (0.002)	−0.94 (−2.09)	0.007 (0.005)	−1.10 (0.63)
Al	0.92 (1.71)	2.54	0.002 (0.002)	−0.18 (1.04)	0.004 (0.002)	−2.03 (−0.91)
TM	0.36 (0.67)	2.54	0.005 (0.007)	−0.03 (−1.19)	0.005 (0.008)	0.54 (−0.40)
Al	1.47 (0.98)	2.88	0.006 (0.007)	−0.05 (−2.59)	0.005 (0.007)	−4.14 (−4.84)
TM	0.64 (0.43)	2.88	0.004 (0.004)	0.05 (0.53)	0.003 (0.002)	−0.67 (1.00)

[16] I. Levi, D. Shechtman, J. Mater. Sci. 27 (1992) 5553.
[17] G.H. Li, D.L. Zhang, H.W. Jiang, W.Y. Lai, W. Liu, Y.P. Wang, Appl. Phys. Lett. 71 (1997) 879.
[18] D. Joseph, S. Ritsch, C. Beeli, New Horizons in Quasicrystals, in: A.I. Goldman, D.J. Sordelet, P.A. Thiel, J.M. Dubois (Eds.), World Scientific, Singapore, 1997, p. 37.
[19] C. Deus, Diploma thesis, TU Dresden, FR Physik, 1996.
[20] Details of the treatment will be presented in a subsequent paper.
[21] S. Braun, Diploma thesis, TU Dresden, FR Physik, 1997.
[22] St. Kek, J. Meyer, Zeitschr. f. Kristallogr. 205 (1993) 235.
[23] D.C. Meyer, K. Richter, B. Wehner, P. Paufler, Philos. Mag. B 77 (1998) 891.
[24] J. Stöhr, Nexafs Spectroscopy, in: Springer, Berlin, 1992, p. 349.
[25] A.G. McKale, B.W. Veal, A.P. Paulikas, S.-K. Chan, G.S. Knapp, J. Am. Chem. Soc. 208 (1988) 3763.